LIGHT SCATTERING IN COMETARY DUST COMAE

GARY HERMAN* and HEIKKI SALO*

Earth and Space Sciences Division, Jet Propulsion Laboratory, Pasadena, Calif., U.S.A.

(Received 28 October, 1986)

Abstract. Detailed single and multiple scattering calculations were carried out for a spherically symmetric cometary atmosphere irradiated by a plane parallel source. Using simplifying assumptions in the single scattering approximation, analytical expressions were derived for the total flux impinging the cometary nucleus, which was shown to be a decreasing function of the coma opacity. Moreover, while highly anisotropic phase functions resulted in more light reaching the nucleus than was the case for isotropic phase functions, the net energy flux at the nucleus surface was still found to be smaller in the presence of a coma than in the no coma case. This increased flux due to the anisotropic phase functions was attributed mostly to the effect of directional scattering in the forward Sun-comet axis. The isotropic multiply scattered flux at the surface was found to be an increasing function of the opacity, τ, for $\tau \lesssim 2.5$. At larger values of τ, the maximum in the downward directed scattered flux was still seen to increase, but occurred at a height of several radii above the nucleus, resulting in a reduction at the surface. On the other hand, the total flux at the surface was again shown to be a decreasing function of τ and always less than in the no coma case. Finally, on comparing the multiply scattered flux with that obtained in the plane parallel approximation, it was quite apparent that except in the vicinity of the Sun-comet axis, the plane parallel geometry tends to underestimate the degree of scattering.

1. Introduction

The cometary nucleus and coma interact in a dynamic way. Sublimation of the icy nucleus carries off the embedded dust giving rise to the observed coma and tail. On the other hand, a dusty cometary atmosphere has been found to modify the heating of the nucleus by effectively increasing the capture cross-section of the photons, some of which will be scattered towards the nucleus, or conversely by attenuating their path (Hellmich and Keller, 1980; Hellmich, 1981; Weissman and Kieffer, 1981, 1984a, b; Marconi and Mendis, 1984).

There are three distinct mechanisms by which the solar flux reaches the nucleus: attenuated direct sunlight, diffuse scattering of the sunlight by the typically micron sized dust particles, and thermal re-radiation by the dust grains in the infrared. Which of the three mechanisms dominates in heating the surface depends on the opacity of the coma, which is a function of the dust to gas ratio, the sublimation rate, and thus the heliocentric distance. For heliocentric distances $r > 1-1.5$ AU, thermal models suggest that the dust production rate is so small that cometary atmospheres are in general optically thin (Hellmich, 1981). Consequently, there will be little or no scattering, and the incoming solar flux will reach the nucleus virtually unattenuated. As the comet approaches closer to the Sun, the opacity of the coma increases, leading possibly to a larger contribution from the scattered and thermally re-radiated fluxes than from the attenuated direct flux (Hellmich, 1981; Marconi and Mendis, 1984).

* NRC Resident Research Associate.

Earth, Moon, and Planets **39** (1987) 51–74.

Following from this, various different approaches have evolved regarding the treatment of the radiation transfer problem in comet thermal models. On the one hand, the presence of the dust coma was neglected (Herman and Podolak, 1985; Fanale and Savail, 1984), on the premise that the increased flux brought about the diffuse radiation fields, more or less compensates for the decreased flux due to the attenuation of the direct radiation. Alternatively, in the nucleus thermal models of Weissman and Kieffer (1981, 1984a, b), the fraction of multiply scattered and thermally re-radiated flux was calculated by using a plane parallel approximation. It should be pointed out however, that a significant fraction of the factor 2.4 increase in the energy flux reaching the nucleus of comet Halley at perihelion, obtained by the above authors, was the result of a numerical error and not the plane parallel approximation (P. Weissman, private communication).

Other work concentrating more on the radiative transfer side of the problem include Squyres *et al.* (1986), who derive an analytical expression for the single scattered flux in a spherically symmetric coma, irradiated by a plane parallel source. Although they take into account the correct geometry describing the radiation field (cylindrical), their solution is valid only in the limit of very small opacities. Their results suggest that the presence of dust leads to a decreased net flux. Hellmich (1981) solves the full multiple scattering problem in cylindrical coordinates based largely on geometrical considerations. He found that the dust halo can increase the total flux reaching the nucleus (neglecting thermal re-radiation) by as much as 1.25. Unfortunately, Hellmich gives little discussion on the role played by his choice of such parameters as the ground albedo or the scattering phase function, making it difficult to establish exact numerical values. Finally Marconi and Mendis (1984) solve the radiative transfer equation in cylindrical symmetry for the Sun-comet axis, to obtain an increased flux of 1.24 for comet Halley at 0.89 AU post-perihelion. In contrast to the above results, this increase was attributed to the thermally re-radiated flux.

Thus it is clear that there exists a wide range of results on the extent to which the coma controls the flux reaching the nucleus. It is therefore our aim to investigate the conditions e.g. coma opacity and scattering phase functions, which result in an increase or decrease in the flux, obtained with the inclusion of a coma over that without. Both single and multiple scattering are treated for the spherically symmetric dust coma. In the case of single scattering we derive simple analytical expressions for the diffuse flux, both for isotropic and nonisotropic phase functions. Although the single scattered flux is not representative of the total diffusive flux for moderate and large τ, it nevertheless gives important insight into the different factors, for example the phase function and the region of scattering in the coma, affecting the amount of light reaching the nucleus. For multiple scattering we apply the moment solution of Wilson and Sen (1980) to generalize the result of Marconi and Mendis (1984) to include all angles of solar incidence. Finally, since most radiative transfer problems have been treated using the plane-parallel approximation, we briefly look at this approximation and compare the results to those obtained in the correct geometry described above.

2. Isotropic Single Scattering

We shall first consider the limit of an optically thin atmosphere, ignoring both multiple scattering and the attenuation of the sunlight. This case has been worked by Squyres *et al.* (1986), to what we shall refer to as the 'zeroth-order' approximation. For convenience, we reproduce the basic assumptions used in obtaining their expression for the isotropically single-scattered flux.

The number density of dust grains is assumed to fall off as $n(r) = n_0 (R/r)^2$, where R is the nucleus radius and r is the radial distance measured from the center of the nucleus. Hence, the velocity of outflow is assumed to be constant with r. The dust is represented by a single characteristic radius, corresponding to an average extinction cross-section, σ. Thus the relation between the incremental optical depth and the geometric distance in the direction of the light ray is $d\tau = \sigma n_0 (R/r)^2 dz$. This allows one to express the total optical depth in the Sun-comet axis as $\tau = n_0 \sigma R$. The flux scattered at a point along the path of the light ray is $\omega S \, d\tau$, where ω is the single scattering albedo and S is the solar flux. However, only a fraction, proportional to the solid angle $d\Omega$ subtended by the nucleus, is scattered in the direction of the nucleus. This was approximately by $d\Omega = \pi R^2/r^2$, so that the probability that a photon will strike the nucleus is $R^2/4r^2$.

The 'zeroth-order' flux scattered in the direction of the nucleus along the ray is given by the equation

$$\Gamma(b) = \int_0^{\tau_\infty} \frac{\omega S R^2 p(\theta) \, d\tau}{4r^2} = \frac{\tau}{4} \omega S R^3 \int_{-\infty}^{\infty} \frac{dz}{(z^2 + b^2)^2}, \tag{1}$$

where we have incorporated the cylindrical coordinates $r^2 = z^2 + b^2$; b representing the impact parameter, while τ_∞ represents the total optical depth of the light ray (Figure 1a). The phase function $p(\theta) = 1.0$ for isotropic scattering. The total flux scattered from all such rays is given by the integral of Equation (1) over all shells of radius b

$$\Gamma^{(0)} = \int_R^{\infty} \Gamma(b) \times 2\pi b \, db. \tag{2}$$

Evaluating Equation (2) and dividing by the surface area of the nucleus we find that

$$F_{\text{cyl}}^{(0)} = \omega S \tau \pi / 16. \tag{3}$$

One drawback of Squyres *et al.*'s. result (Equation (3)), is that it neglects scattering in the 'forward shadow' region (Figure 1a). This led us to consider the additional contribution to the diffuse flux from the single scattering originating in the sun-comet axis. On solving Equations (1)–(3) in spherical polar rather than cylindrical coordinates, we obtain the 'zeroth-order' spherical approximation to the diffuse flux

$$F_{\text{sph}}^{(0)} = \frac{1}{4\pi R^2} \times \frac{\tau \omega S R^3}{4} \int_0^{\pi} 2\pi \sin \Theta \, d\Theta \int_R^{\infty} \frac{dr}{r^2} = \omega S \tau / 4. \tag{4}$$

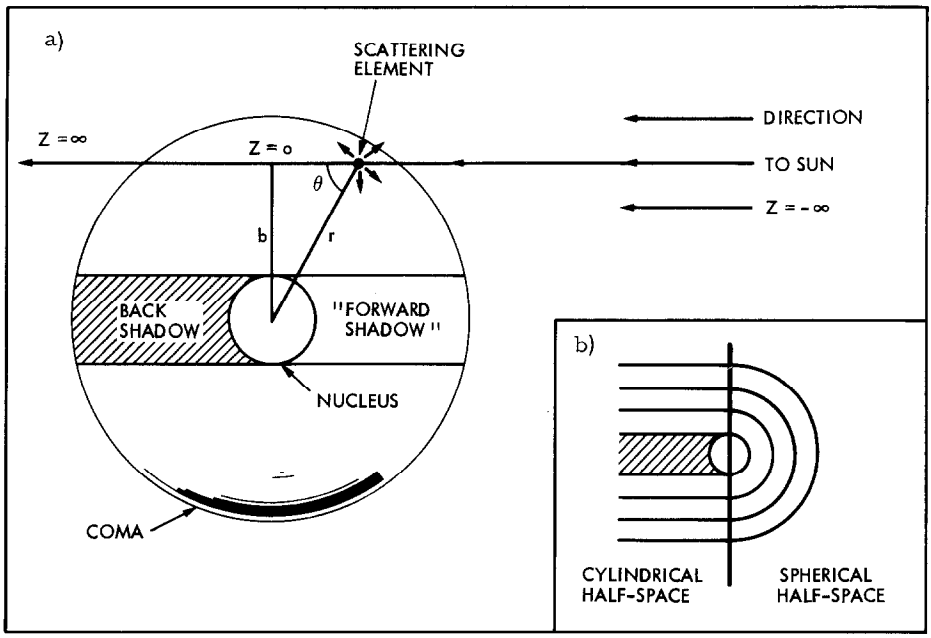

Fig. 1. (a) The coordinate system used in the calculation of the zeroth and first order single scattered flux. (b) The division of the spherically-symmetric coma into the Sun-facing 'spherical half-space', and the back-side 'cylindrical half-space'.

Therefore the inclusion of the Sun-comet axis increases the flux by a factor of $4/\pi$. However, $F^{(0)}_{\text{sph}}$ includes incorrectly the scattering behind the nucleus which in the optically thin limit is zero. From Figure 1b it is clear that for small τ the corrected 'zeroth order' flux is simply the average of $F^{(0)}_{\text{cyl}}$ and $F^{(0)}_{\text{sph}}$: i.e.,

$$\bar{F}^{(0)} = \omega S \frac{\tau}{8}\left(\frac{\pi}{4} + 1\right). \tag{5}$$

As one would expect, in the optically thin limit the flux varies linearly with τ (see Table I). We shall return to discuss this result in the light of the higher order approximations that follow.

A second minor modification comes from the adopted form of the solid angle. Although computationally convenient, it breaks down for small r ($r \lesssim 2R$). The solid angle is more accurately expressed as $2\pi[1 - (1 - (R/r)^2)^{1/2}]$ (Hellmich, 1981). Using this latter form, the flux given by Equation (5) can be shown to be increased by approximately 6%. Since it is our aim to present, whenever possible, simple analytical expressions for the single scattered flux, we shall assume Squyres *et al.*'s. (1986) form for the solid angle. However, the 6% correction factor will be incorporated into the expression for the total flux given at the end of this section.

TABLE I

Zero and first order isotropically single scattered flux as a function of τ as defined in Equations (5) and (9) respectively. The last two columns show the isotropic single scattered flux computed from Equations (A1)–(A7) and from the moment equations (27)–(29), respectively. The factors ωS is taken to be unity, and all fluxes must be multiplied by 10^{-2}.

τ	$\bar{F}^{(0)}$	$\bar{F}^{(1)}$	$\bar{F}_{ss}$	F_{ss}
0.01	0.223	0.221	0.23	0.22
0.05	1.116	1.078	1.10	1.05
0.10	2.232	2.074	2.04	2.04
0.15	3.348	3.000	2.85	2.84
0.20	4.463	3.857	3.53	3.56
0.25	5.579	4.656	4.11	4.18
0.30	6.695	5.410	4.60	4.73
0.35	7.811	6.099	4.99	5.20
0.40	8.927	6.745	5.32	5.59
0.45	10.043	7.348	5.58	5.93
0.50	11.159	7.912	5.78	6.19

So far attention has been concentrated on the corrections arising from geometric factors ('forward-shadow' region and solid angle). A final factor that must be considered is the dependence of the flux on the radial distribution of the dust. It turns out that with the inclusion of the hydrodynamically calculated velocity of outflow (Divine, 1981), the number density falls off somewhere in the range $1/r^2$ to $1/r^3$. However, using a $1/r^3$ distribution for a fixed optical thickness, results in no change in the flux if the Sun-comet axis is excluded, and a 15% decrease with the inclusion of the 'forward shadow' region. Since we are interested in the maximum possible flux reaching the nucleus we shall restrict our study to the $1/r^2$ distribution.

When calculating the single scattered flux for larger opacities, the attenuation (extinction) of the incident beam before scattering must also be taken into account. The attenuation of the incident ray through a dust column with optical depth τ_d, can be expressed as $S - \rightarrow S \exp(-\tau_d)$. Integration along the light path gives the attenuation of the beam at a point (z, b)

$$\mathrm{S}\exp\left[-R^2 n_0 \sigma \int_{-\infty}^{z} [\mathrm{d}z'/9z'^2 + b^2)]\right] = \mathrm{S}\exp\left[-u\left(\arctan\left(\frac{z}{b}\right) + \frac{\pi}{2}\right)\right], \tag{6}$$

where $u = \tau R/b$. Substitution (6) into Equation (1) we obtain

$$\Gamma^{(1)}(b) = \frac{\tau}{4}\,\omega S R^3 \int_{-\infty}^{\infty} \frac{\exp\left[-u(\arctan(z/b) + (\pi/2)\right]\,\mathrm{d}z}{(z^2+b^2)^2}, \tag{7}$$

which is readily integrated to give

$$\Gamma^{(1)}(b) = \frac{\omega S R^2}{2b^2} \frac{(1-e^{-u\pi})}{(u^2+4)}. \tag{8}$$

Excluding the backward shadow region, Equation (8) was integrated over all shells of radius b to give

$$\bar{F}^{(1)} = \frac{\omega S}{8}\left[\int_0^{\tau} \frac{e^{-u\pi/2}}{u(u^2+4)}(u^2-2(e^{-u\pi/2}-1))\,du + \int_0^{\pi/2}(1-e^{-\tau x/\sin x}) \times \right.$$

$$\left. \times \frac{\sin 2x\,dx}{2x}\right]. \tag{9}$$

It is easily verified that in the limit as $\tau \to 0$ Equation (9) simplifies to give Equation (5). Equation (9) was evaluated numerically, and compared (see Table I) to the zero order flux derived earlier. It is clear from the Table that as τ increases, the incident beam is increasingly attenuated, so that $F^{(0)} > F^{(1)}$. In fact, on including the attenuation of the beam before scattering, the scattered flux is reduced by 30% at $\tau = 0.5$. It would, therefore, seem logical also to include the attenuation of the scattered beam, in order to obtain the 'true' single scattered flux, $\bar{F}_{ss}$. However, the simple geometric approach that has been followed until now can no longer be applied, since the optical path after scattering depends on where the light strikes the nucleus. We have, therefore, adopted the method whereby the light ray from each scattering element in the coma, is traced to discrete surface elements on the nucleus surface (see Appendix A). This method, besides correctly including the attenuation before and after scattering, also automatically takes into account the correct solid angle, and excludes the backward shadow region. Furthermore, it is not restricted to any simplifying assumption for the phase function. The fourth column in Table I gives $\bar{F}_{ss}$ calculated in the way described in Appendix A. As one would expect $\bar{F}_{ss} < \bar{F}^{(1)}$, especially at large τ where there is greater attenuation of the scattered beam.

Leaving for a moment the treatment of the scattered flux, we turn our attention to the attenuated direct sunlight, given by the Equation $F_{\text{dir}} = (Se^{-\tau}/4)$. According to Equation (6), the attenuation of the tangential light ray ($z = 0$, $b = R$) is $e^{-\pi\tau/2}$. Therefore, independent of the nucleus radius the optical depth to the edge of the nucleus is a factor of $\pi/2$ larger than to the center. Hence, a large fraction of the Sun-facing hemisphere is shielded by a substantially thicker dust blanket than implied by τ. This effect will be most important for moderate values of τ. The correct direct flux at the surface per unit area is given by

$$\bar{F}_{\text{dir}} = \int_0^{\pi/2} S\, e^{-\tau(\Theta)} \cos\Theta \times 2\pi R^2 \sin\Theta\, d\Theta/4\pi R^2 =$$

$$= \int_0^1 \frac{S}{2} \exp\left[-\frac{\tau}{\mu}\left(\frac{\pi}{2} - \arccos\mu\right)\right] \mu\, d\mu, \tag{10}$$

TABLE II

The corrected direct flux $\bar{F}_{dir}$ as given in Equation (10) compared with $F = (1/4)e^{-\tau}$

τ	F	$\bar{F}_{dir}$	$\bar{F}_{dir}/F$
0.1	0.2262	0.2231	0.986
0.5	0.1516	0.1415	0.933
1.0	0.0920	0.0804	0.874
1.5	0.0558	0.0458	0.821
3.0	0.0125	0.0086	0.691

where $\mu = \sin\theta$. For example, if $\tau = 1$, $\bar{F}_{dir}$ is about 13% smaller than F_{dir} (Table II).

We can now evaluate the effects of the dust on the total flux received by the nucleus in the limit of small τ. In this limit Equation (10) simplifies to

$$\bar{F}_{dir} \approx \frac{S}{4}(1-(\pi-2)\tau). \tag{11}$$

Combining this with the single-scattered flux given by Equation (5) corrected for the solid angle, we find that

$$F_T \approx \frac{S}{4}[1-(1.14-0.95\ \omega)\tau] + F_{rr}\ , \tag{12}$$

where F_{rr} denotes the thermally re-radiated flux. Hence, it can be seen that even for conservative scattering ($\omega = 1$, $F_{rr} = 0$), F_T is a decreasing function of the opacity of the coma. In the more general case of $\omega < 1$, the probability that a photon is absorbed by the dust grains is given by $(1 - \omega)$. If we assume the emissivity $\epsilon = 1$, all absorbed radiation will be isotropically thermally re-radiated at infrared wavelengths. In the limit of small τ the probability of striking the nucleus is, therefore, the same for the thermally re-radiated and the scattered visible radiation. Hence, the decrease in the latter contribution is exactly compensated for by the inclusion of the thermal re-radiation. Therefore, the total flux is independent of ω, and is obtained by setting $\omega = 1$ ($F_{rr} = 0$) in Equation (12).

3. Anisotropic Single Scattering

We now turn our attention to anisotropic scattering while remaining in the single scattering approximation. The Henyey–Greenstein phase function is most commonly used to represent scattering from non-spherical particles. It takes the form

$$p(\mu) = (1 - g^2)/(1 + g^2 - 2g\ \mu)^{3/2}, \tag{13}$$

where $-1 < g < 1$, and μ is the cosine of the angle between the direction of the initial and emerging light ray. However, as will be demonstrated below, Equation (13) can be approximated for a restricted range of g, by the computationally convenient

truncated Legendre polynomial expansion (Euler phase function)

$$p(\mu) = 1 + X\mu. \tag{14}$$

From the definition of the anisotropic factor

$$g = \tfrac{1}{2} \int_{-1}^{1} p(\mu)\mu \, d\mu,$$

the Legendre coefficient $X = 3g$. Since $p(\mu)$ is non-negative, X must be less than 1.0 or $g < 1/3$, if this truncated expansion is to be used. However, micron-sized silicate dust grains are strong forward-scatterers with an anisotropic factor $g \approx 0.7$ (Weissman and Kieffer, 1984a; Marconi and Mendis, 1984).

If we substitute the above equations into Equation (1), analytical integration of Equation (13) is only possible over the Sun-facing hemisphere, which when carried out yields

$$F = \omega S \frac{\tau}{8} [1/g + 1 - (1-g^2)/g(1+g^2)^{1/2}]; \tag{15}$$

while the Euler function integrated over the same region, yields

$$F = \omega S \frac{\tau}{8} [1 + 3g/2]. \tag{16}$$

For $g = 0.1$ and 0.3, Equation (16) overestimates the flux by a factor of 1.001 and 1.015, respectively. Moreover, while Equation (16) is not strictly valid for $g = 0.7$, the flux is overestimated by only 12%. Therefore, in order to obtain closed analytical expressions for the nonisotropic flux, we shall assume the Euler phase function given by Equation (14). However, it must be kept in mind that this represents an upper bound on the impinging flux at the nucleus.

Squyres *et al.* (1986) found that in the optically thin limit, the anisotropic contribution to the flux cancels, because of the assumed cylindrical symmetry. However, if we take into account the asymmetry introduced by the 'forward shadow' region (Figure 1b), the 'zero-th order' order flux becomes

$$\bar{F} = \omega S \frac{\tau}{8} [\pi/4 + 1 + g/2]. \tag{17}$$

Hence, the important contribution to the diffuse flux arising from the 'forward shadow' region $\omega S \tau X/48$ manifests itself.

Following along the same lines as the isotropic studies, we now consider larger optical depths, so that the attenuation of the initial beam must also be taken into account. The additional term to Equation (7) arising from the anisotropic factor is $X\, G^{(1)}$, where

$$G^{(1)} = \frac{\tau}{4} \omega S R^3 \int_{-\infty}^{\infty} \exp\left[-u\left(\arctan\left(\frac{z}{b}\right) + \frac{\pi}{2}\right)\right] \frac{z \, dz}{(z^2+b^2)^{5/2}}. \tag{18}$$

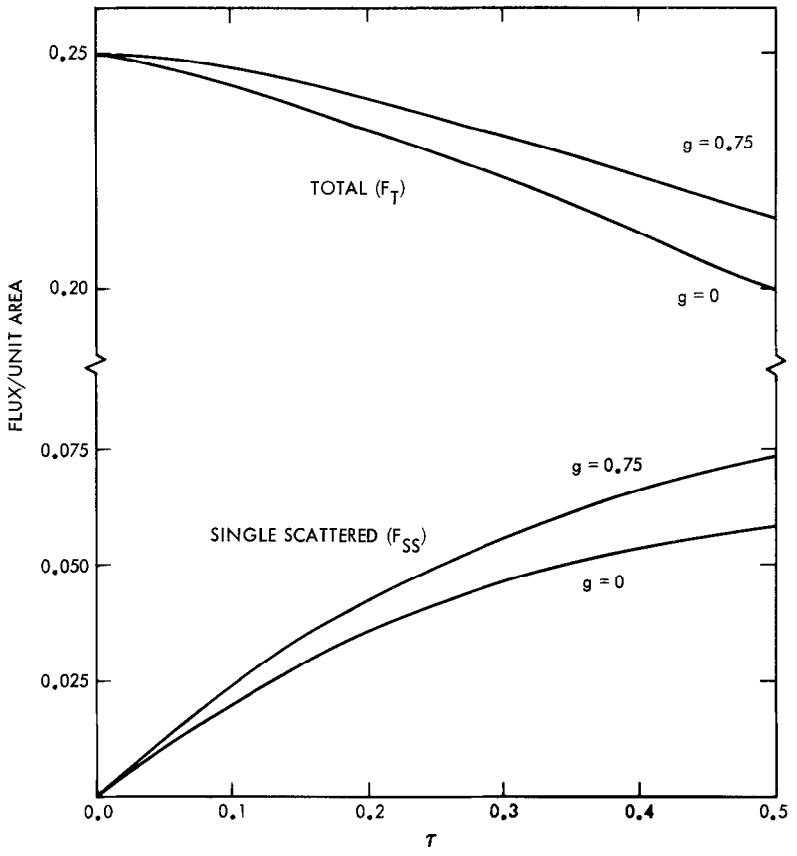

Fig. 2. The single scattered and total flux impinging the nucleus as a function of the optical depth, τ, for an isotropic and a highly forward scattering Henyey–Greenstein phase function. Conservative scattering ($\omega = 1$) was assumed.

The integration over dz can be done analytically, after which the integration over the impact parameter b leads to the expression

$$\bar{G}^{(1)} = \frac{\omega S}{8}\left[\int_0^{\tau} \frac{2ue^{-u\pi} - (3+u^2)e^{-u\pi/2}}{(1+u^2)(9+u)^2}\,\mathrm{d}u + \int_0^{\pi/2}(1-e^{-\tau x/\sin x}) \times \right.$$

$$\left. \times \frac{\sin^2 x \cos x\,\mathrm{d}x}{x}\right], \tag{19}$$

where as before, $u = \tau R/b$. Combining this with Equation (9) we obtain the 'first-order' anisotropically-scattered flux.

The 'zeroth-and first-order' anisotropic terms are given in Table III. Note that the attenuation of the flux in $G^{(1)}$ is not symmetrical with respect to the Sun and anti-Sun facing directions. Consequently, adding the positive and negative contributions

TABLE III

The non-isotropic contribution to the zeroth and first order single scattered flux as a function of τ, as defined in Equations (17) and (19). The factor ωS is taken to be unity, and all terms must be multiplied by the factor $X\ 10^{-2}$.

τ	$\tau/48$	$\bar{G}^{(1)}$
0.01	0.021	0.021
0.05	0.104	0.107
0.10	0.208	0.217
0.15	0.312	0.331
0.20	0.417	0.446
0.25	0.521	0.561
0.30	0.625	0.676
0.35	0.729	0.791
0.40	0.833	0.905
0.45	0.937	1.015
0.50	1.042	1.125

to the anisotropic part of the flux, we obtain a slightly larger value than was found for the zeroth-order case.

Analogously to Equation (12), the total flux for anisotropic scattering in the limit of small τ is given by

$$F_T \approx \frac{S}{4}\,[1-(0.19-(0.265\,g\omega)_\tau],\tag{20}$$

where we have assumed the Euler phase-function, and the thermal re-radiation is incorporated by the way described at the end of Section 2. For $g < 0.5$ the total flux is only slightly overestimated over that which would be obtained on using the Henyey–Greenstein phase function. However, the use of the latter function results in a decrease in F_T with τ for all g (Figure 2), contrary to Equation (20) which shows an increase in F_T for $\omega g > 0.74$. It is clear from the figure that $\bar{F}_{ss}$ and, therefore, also F_T increases as a function of g. For example at $\tau = 0.5$ and $g = 0.75$, $\bar{F}_{ss}$ and F_T are increased by about 25% and 8% respectively over the isotropic case. This increase however is still insufficient to reverse the trend of F_T decreasing with τ.

4. Multiple Scattering

For moderate to larger values of τ, the single scattering approximation fails. The optically thicker atmosphere means that there will be a larger number of scattering centers, so that the light ray may change its direction many times before its path intersects the nucleus.

We therefore solved the full radiative transfer equation for a spherically-symmetric atmosphere illuminated by parallel solar rays. The equation is given (cf. Sobolev,

1975, p. 219) by

$$\mu \frac{\partial I}{\partial r} + \frac{1-\mu^2}{r} \frac{\partial I}{\partial \mu} + \frac{(1-\mu^2)^{1/2}}{r} \cos \phi \frac{\partial I}{\partial \psi} - \frac{\cot \psi \, (1-\mu^2)^{1/2}}{r} \sin \phi \frac{\partial I}{\partial \phi} =$$

$$= \alpha(r)(B-I), \tag{21}$$

where the source function $B(r, \psi, \theta, \phi)$ is given by

$$B = \frac{\omega}{4\pi} \int_0^{2\pi} d\phi' \int_0^{\pi} I(r, \psi, \Theta', \phi') \, P(\delta') \sin \Theta' \, d\Theta' + \frac{\omega}{4} SP(\delta) e^{-T}; \tag{22}$$

where $I(r, \psi, \theta', \phi')$ is the intensity, $\mu = \cos \theta$, and r, ψ are the spherical coordinates of the point in the atmosphere, for which ψ is the angle between the radius vector of the point and the direction towards the Sun. Note that ψ now corresponds to the spherical angle which was denoted by θ in Section 2. Following Sobolev, we denote the incident radiation at the top of the atmosphere by πS, in place of S, used in the previous sections; $\alpha(r)$ is the absorption coefficient, and ω is the grain single scattering albedo. The phase function for scattering between the (θ', ϕ') and (θ, ϕ) directions is $P(\delta') = 1 + X \cos \delta'$, where $\cos \delta' = \cos \theta \cos \theta' + \sin \theta \sin \theta' \cos(\phi - \phi')$, and X is related to the anisotropic factor (see Equation (14)).

The optical depth T, measured from the outer surface to the point in the atmosphere is given by

$$T = \int_{r \sin \psi}^{(R_1^2 - r^2 \sin \psi)^{1/2}} \alpha(r') \, dz' \tag{23}$$

where R_1 is the outer limit of the dust envelope. By assuming $\alpha(r)$ to vary as $1/r^2$, Equation (23) can be integrated to give

$$T = \alpha(r)/(r \sin \psi) \, [\arctan(R_1/r \sin \psi) + \psi - \pi/2]. \tag{24}$$

The above expression is analogous to Equation (6) in the single-scattering approximation.

Wilson and Sen (1980) developed an approximate technique for solving the complex integro-differential equations (21) and (22), by taking their appropriate moments and representing the radiation field by three streams, with each stream averaged over μ. On the basis of the shadowing effect of the nucleus, the intensities were defined as

$$I = I_n(r, \psi) + f(r, \psi) \cos \phi; \quad n = 1, 2, 3 \tag{25}$$

for the three regions $\mu_r \leq \mu \leq 1$, $0 < \mu < \mu_r$, and $-1 \leq \mu \leq 0$, respectively, where

$$\mu_r = [1 - (R/r)^2]^{1/2}. \tag{26}$$

The multiple scattered flux per unit area F_{ms} is, therefore, the average of I_3–the downward directed intensity over the surface area of the nucleus. Substituting Equation (25) into the appropriate moment equations, Wilson and Sen (1980) derived a closed system of four partial differential equations

$$\frac{\partial H}{\partial r} + \frac{2H}{r} + \frac{\pi}{8r}\left(\frac{\partial f}{\partial \psi} + f \cot \psi\right) = \alpha(\omega - 1) J + \frac{1}{4}\alpha\omega Se^{-T}, \quad (27)$$

$$\frac{\partial K}{\partial r} + \frac{1}{r}(3K - J) = -\alpha H - \alpha \frac{\omega X}{3}\left[\frac{\cos \psi Se^{-T}}{4} - H\right], \quad (28)$$

$$\frac{\partial}{\partial r}[\mu_r(3K - J) + 2H] + \frac{4\mu_r}{r}(3K - J) + \frac{\pi}{8r}\left(\frac{\partial f}{\partial \psi} + f \cot \psi\right) =$$

$$= -4\alpha K + \frac{4\alpha\omega}{3}\left(J + \frac{Se^{-T}}{4}\right), \quad (29)$$

$$\frac{1}{r}\frac{\partial}{\partial \psi}[J - K] = -\frac{\pi\alpha f}{4}\left[1 - \frac{\omega X}{3}\right] + \frac{\alpha\omega X}{12}\sin \psi\, Se^{-T}, \quad (30)$$

where the moment J, H, and K are defined

$$J = \int I \mathrm{d}\omega/4\pi; \quad H = \int I\,\mu\,\mathrm{d}\omega/4\pi; \quad K = \int I\mu^2\,\mathrm{d}\omega/4\pi. \quad (31)$$

The boundary conditions are:

(i) the downward-directed diffuse radiation I_3 at the outer boundary of the coma is zero. Writing I_3 in terms of the above moments J, H, and K, we obtain

$$\mu_r J + 3K - 2(1 + \mu_r)H = 0; \quad (32)$$

(ii) the diffuse radiation reflected back to the medium at the inner boundary (surface), is given by the albedo A times the downward-directed flux. This leads to

$$J + 2H = A(J - 2H + S \cos \psi\, e^{-T}) \quad \text{and} \quad K = J/3. \quad (33)$$

On the basis of the latter boundary condition, Wilson and Sen (1980) approximated the moments J, H, and K, to obtain with the aid of Equation (30), a closed expression for f, of the form

$$\frac{\pi}{4}(3 - \omega X)f = \frac{\omega X}{2}\sin \psi\, Se^{-T} + \frac{ASe^{-T}}{\alpha r}\left[\sin \psi + \cos \psi \frac{\partial T}{\partial \psi}\right]. \quad (34)$$

However, on substituting Equation (24) into (34) it was found that, at the outer boundary R_1, Equation (34) becomes unbounded. The above authors, and more

recently Wilson and Wan (1983), did not encounter this problem because they studied an atmosphere whose extent was very small compared to the nucleus radius. Even for this case, a close inspection of Table I of Wilson and Sen (1980) discloses unphysical fluctuations in the intensity with increasing r for a nonzero ground albedo. Marconi and Mendis (1984), chose to solve the above system of equations in the Sun-comet axis ($\psi = 0$), where the rotational symmetry of the radiation field about this axis implies that $f = 0$. It does not imply, however, as assumed by the authors, that $\partial f/\partial\psi + \cot\psi \cdot f = 0$ (Equations (27) and (29)). This becomes evident in the limit $R_1 \to \infty$, where we can approximate Equation (24) by

$$T = \alpha(r) r\psi/\sin\psi. \tag{35}$$

Substituting Equation (35) into (34), and letting $\psi \to 0$, we obtain

$$\frac{\pi}{8r}\left(\frac{\partial f}{\partial\psi} + f\cot\psi\right) = \frac{Se^{-T}}{\alpha r(3-\omega X)}\left[\frac{\omega X}{2} + \frac{2A}{\alpha r}\right]. \tag{36}$$

The factor $1/\alpha r$ in the last term of Equation (36), makes the latter to diverge even faster than Equation (34). It would, therefore, appear that the definition of the intensity given by Equation (25) contains an inherent singularity. In order to avoid this singularity, we chose the ground albedo $A = 0$ and considered only isotropic scattering – i.e., $X = 0$. This suppresses the right-hand side of Equations (34) and (36) to zero. Equations (27)–(29) are now of the same form assumed by Marconi and Mendis (1984), and can be used to calculate the impinging flux as a function of ψ. Fortunately, very small albedos have recently been reported for cometary nuclei, typically less than 0.1 (e.g. for Halley $A = 0.04$; cf. Keller *et al.*, 1986); so that the restriction on the albedo is not critical for our purposes (see Appendix B). The effects of anisotropic scattering will be discussed at the end of this section.

As a first check of the method we neglected the multiple scattering term in the source function of Equation (22), and compared the single scattered flux F_{ss} to the numerically-integrated flux given in Appendix A. The results are presented in the last two columns of Table I. We see that there is very good agreement between the two methods differing by at most 7% at $\tau = 0.5$. This was also found to be true for the distribution of the flux with ψ.

We now turn to the full solution of the moment Equations (27)–(29). The variation in I_3 at the surface as a function of ψ is shown in Figure 3. It can be seen that for small τ, I_3 is nearly constant with ψ, only significantly diminishing close to the shadow region behind the nucleus. For larger opacities the diffuse radiation decreases more rapidly with increasing ψ. This is a consequence of the fact that for larger ψ, the light must travel further before it is scattered towards the nucleus, so that it is more strongly attenuated. Nevertheless, the 'dark-side' of the nucleus is still heated as a result of the diffuse radiation fields, an effect which would not be observed in the absence of a coma. It is interesting to note that at $\tau = 3.0$, I_3 at the surface is smaller than at $\tau = 2.0$ for all ψ. This effect can also be seen in Figure 4, which shows the behaviour of I_3 versus height above the nucleus for $\psi = 0°$, $60°$

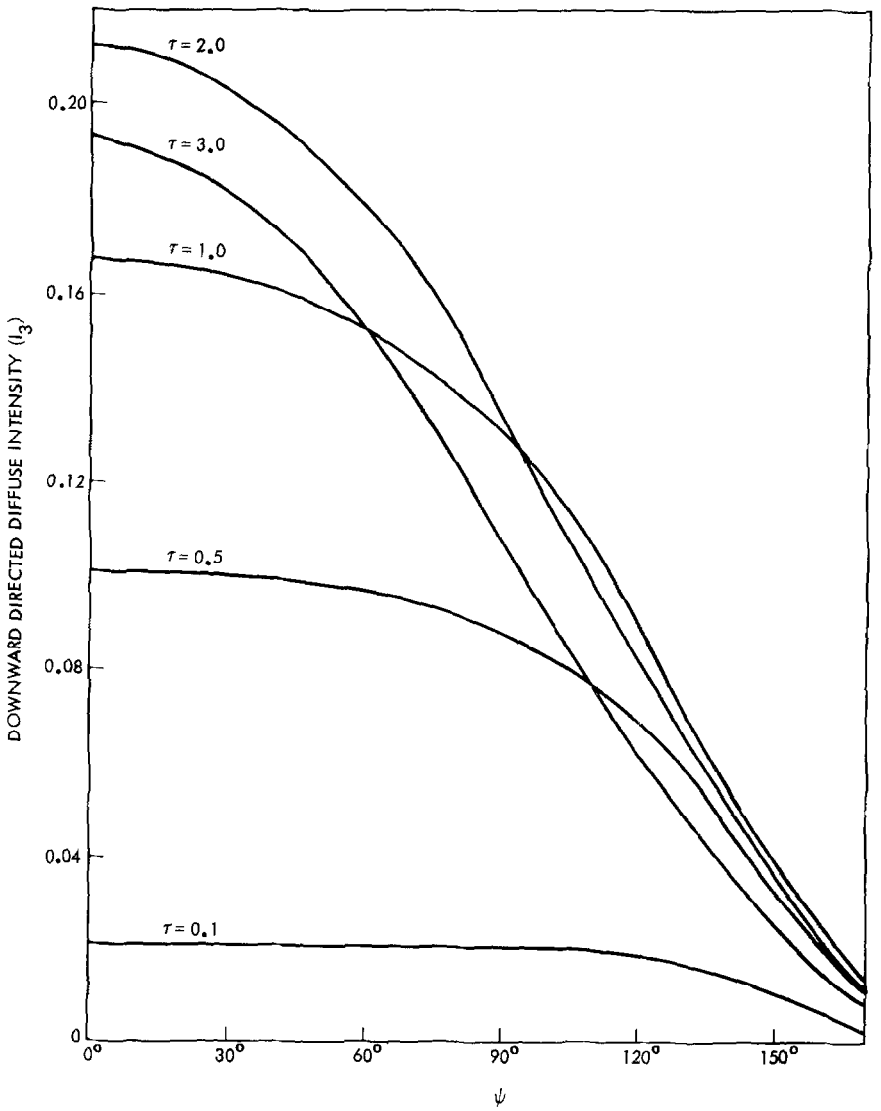

Fig. 3. The downward directed diffuse radiation I_3 at the surface as a function of ψ and τ, obtained from the moment equations (27)–(29), for $g = A = 0$ and $\omega = 0.9$.

and 120° at $\tau = 3.0$, as well as for $\psi = 0°$ at $\tau = 2.0$. In the first case, the maximum in I_3 occurs at an altitude of approximately $1.6R$ at $\psi = 0°$, increasing to a height of approximately $2.5R$ at $\psi = 120°$. This behavior results from the increased attenuation of the incident beam with increasing ψ, as mentioned previously, as well as the shadowing effect of the coma by the nucleus for $\psi > 90°$. Furthermore, at $\psi = 0°$ it can be seen that the maximum in I_3 is greater for $\tau = 3.0$ than for $\tau = 2.0$. Hence, it is quite apparent that although the maximum in I_3 increases with τ, it occurs at a greater height above the nucleus, resulting in a smaller heat flux at the surface.

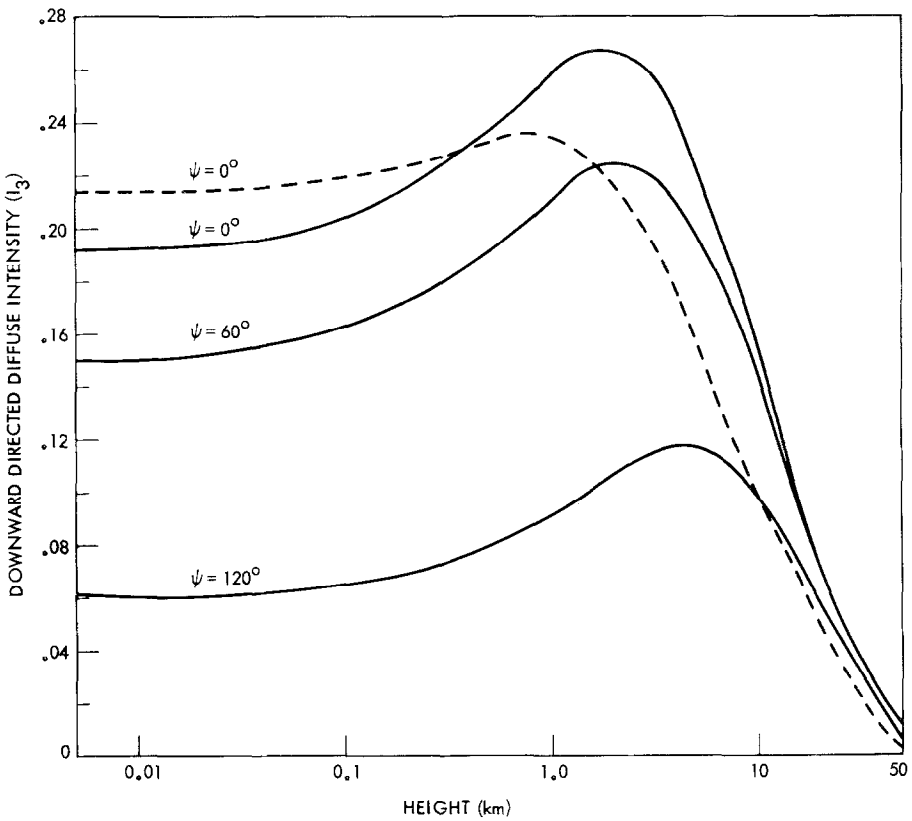

Fig. 4. I_3 as a function of height above the nucleus for different values of ψ, obtained from the moment equations (27)–(29). The solid lines represent $\tau = 3.0$ and the dashed line $\tau = 2.0$. ($g = A = 0$, $\omega = 0.9$).

The distribution of the total energy flux on the nucleus surface as a function of ψ for the case of isotropic conservative scattering is presented in Figure 5. In the no coma case ($\tau = 0$), the flux simply varies as cos ψ. With increasing opacity, multiple scattering tends to dominate over the attenuated direct flux, re-distributing more energy to the unilluminated side of the nucleus. Thus the effect of an optically thick coma on the energy flux reaching the nucleus is not only to diminish it, but also to make the surface more isothermal.

For non-conservative scattering, we must also include the contribution from the thermal re-radiation. In the Marconi and Mendis (1984) solution, a small but non-zero infrared opacity was assumed. Subsequently, they solved the same set of Equations (27)–(29) after replacing the source function with the appropriate black body radiation term. However as briefly described in Section 2, we have assumed that all the visible radiation absorbed is subsequently emitted isotropically at infrared wavelengths greater than the average grain size. Consequently, it will undergo only a negligible amount of attenuation after scattering before reaching the nucleus. This simplifies the calculation as follows. The amount of absorbed radiation for each

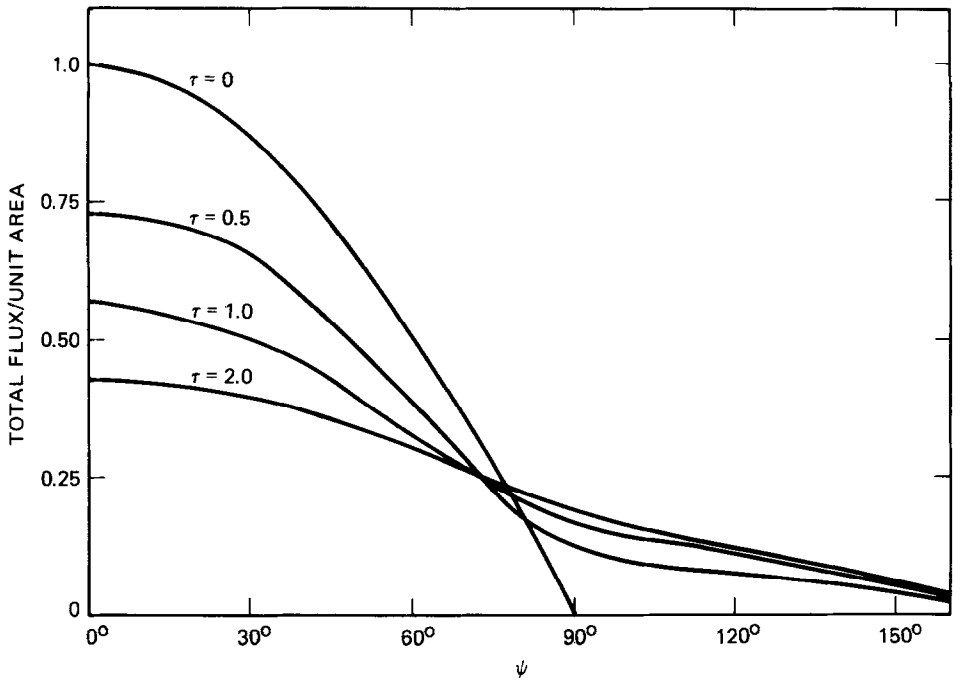

Fig. 5. The distribution of the total energy flux on the nucleus surface as a function of τ and ψ for isotropic conservative scattering.

volume element in the coma is multiplied by the probability that the re-radiation is directed towards the nucleus and then integrated over the entire coma. This leads to

$$F_{rr} = \frac{(1-\omega)}{4\pi R^2} \int \int \int \pi \, (Se^{-T} + J) \, \frac{(1-\sqrt{1-(R/r)^2})}{2} \, \alpha \, \mathrm{d}V, \tag{37}$$

where we have incorporated Hellmich's (1981) form for the solid angle, and α $\mathrm{d}V = r^2 \sin\psi \, \mathrm{d}\psi \, \mathrm{d}\tau \, \mathrm{d}\phi$. The terms $\pi S e^{-T}$ and πJ correspond to the absorbed direct and diffuse radiation (Equation (31)), respectively.

The behaviour of the isotropically multiple scattered, thermally re-radiated, and attenuated direct fluxes; F_{ms}, F_{rr}, and $\bar{F}_{\mathrm{dir}}$, respectively, as well as the total flux with and without a coma, are shown in Figure 6 as a function of τ for $\omega = 0.9$. Also shown is the 'first-order' single scattered flux $\bar{F}^{(1)}$, where it will be recalled that the attentuation of the scattered beam was neglected. It is immediately evident from the figure that for the chosen set of parameters, $F_{\mathrm{ms}} > \bar{F}_{\mathrm{dir}}$ for $\tau > 0.8$, and $F_{\mathrm{rr}} > \bar{F}_{\mathrm{dir}}$ for $\tau > 1.8$. The smaller contribution from F_{rr} is a consequence of the large single scattering albedo. Most importantly, the sum of all three terms which gives the total flux was always less than that obtained in the case of no coma.

Finally, it is interesting to note that F_{ms} is closely approximated by $\bar{F}^{(1)}$ for all $\tau < 2.0$. In other words, the neglect of the attenuation of the scattered beam after a single-scattering event, closely mimics multiple scattering. However for $\tau > 2.0$, $\bar{F}^{(1)}$

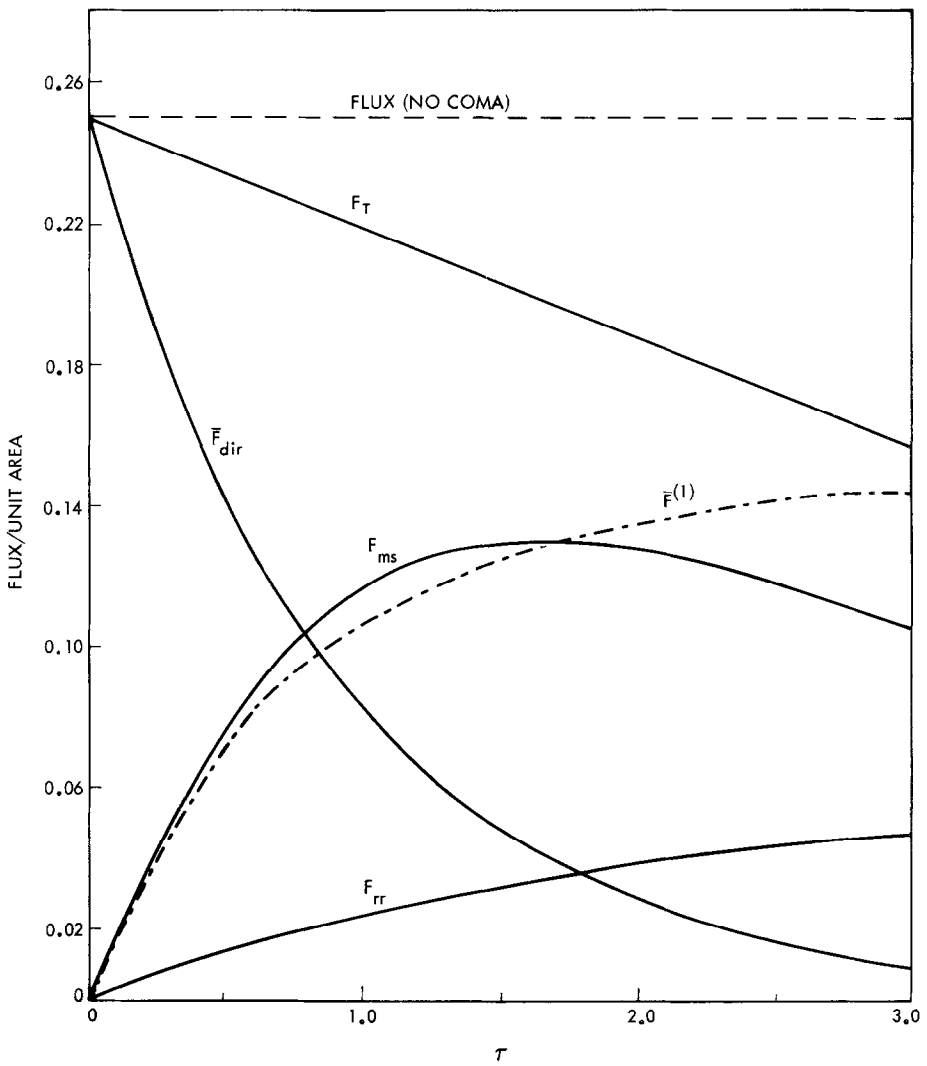

Fig. 6. The multiply-scattered, thermally re-radiated and attenuated direct flux, F_{ms}, F_{rr}, and $\bar{F}_{dir}$ ($g = A = 0, \omega = 0.9$) as a function of τ. Also shown is the total flux with and without a coma, and the 'first order' single scattered flux $\bar{F}^{(1)}$.

continues to increase monotonically, whereas F_{ms} reaches a maximum and then declines. In addition, for small τ the second term in Equation (37) is much smaller than the first term, so that Equation (37) can be approximated by scaling $\bar{F}^{(1)}$ given by Equation (9) by $(1 - \omega)$ in place of ω. Therefore, as was observed in the case of isotropic single scattering, the thermal re-radiation and the isotropic multiple scattering tend to compensate each other.

As we have stated, the above the results strictly apply to isotropic scattering in the case of zero ground albedo. It was later found through Monte Carlo simulations (to

be discussed in a future publication) that for $g = 0.75$, F_{ms} was increased by $\sim 25\%$, however still not enough for the total flux to be greater than in the no coma case.

5. Plane-Parallel Approximation

The complexity of the calculations in Section 4 arose as a result of the dependence of the intensity on the two spatial and two angular variables r, ψ, θ, ϕ. In comparison, the azimuth-independent intensity in the plane parallel geometry is simply $I(\mu, \mu_0)$, where μ_0 is the cosine of the solar zenith angle (denoted by ψ in Section 4). This greatly simplifies the solution of the radiative transfer equation, and it is for this reason that most of the work on planetary atmospheres has been based on this approximation (Irvine, 1975). In fact, Sobolev (1971) argues that if the extent of the atmosphere is very small compared to the curvature of the planet, a plane-parallel-layered atmosphere can be applied provided that the angle of illumination is adjusted for the sphericity of the atmosphere. In the case of comets this condition is less likely to be satisfied. However, it is still of interest to study the applicability of the plane-parallel approximation in the light of the results in Section 4.

The azimuthally-averaged form of the transfer equation, describing the intensity $I(\tau, \mu)$ is of the form

$$\mu \frac{dI}{d\tau} = -I + \frac{\omega}{2} \int_{-1}^{1} P(\mu, \mu') I(\tau, \mu') \, d\mu' + \frac{\omega S}{4} P(\mu, \mu_0) e^{-\tau/\mu_0}, \tag{38}$$

where (as defined earlier) ω is the single-scattering albedo, μ and μ_0 are the cosine of the emergent and solar zenith angles, respectively; $P(\mu, \mu')$ is the azimuthally averaged scattering phase function for light incident at μ' and scattered in the direction μ; and πS is the incident solar flux. Equation (38) was solved with the aid of the Eddington approximation, which assumes that the intensity can be expressed as $I(\tau, \mu) = I_0(\tau) + I_1(\tau)\mu$. The solution to Equation (38) is given in Equations (12)–(14) of Shettle and Weinman (1970). Although the Eddington approximation is slightly less accurate than the more involved higher-order approximations such as the 4-stream (Liou, 1974), it is sufficiently accurate for our purpose. In general, it turns out that close to the Sun-comet axis ($\mu_0 = 1$) the plane parallel approximation overestimates the flux; while for $\psi > 30°$ it tends to underestimate the flux. For small τ, these differences partially compensate each other if the multiply-scattered flux is integrated over ψ. Thus, in order to obtain an estimate for the multiply-scattered flux averaged over the surface, the spherical coma was replaced locally with a plane parallel atmosphere of the same total optical depth, illuminated from the appropriate directions. It is clear from Figure 7 curves (c) and (d), that for $\tau > 0.25$ the plane parallel approximation underestimates the scattered flux. A slightly better approximation to F_{ms} was obtained by choosing a suitable μ_0 to represent the

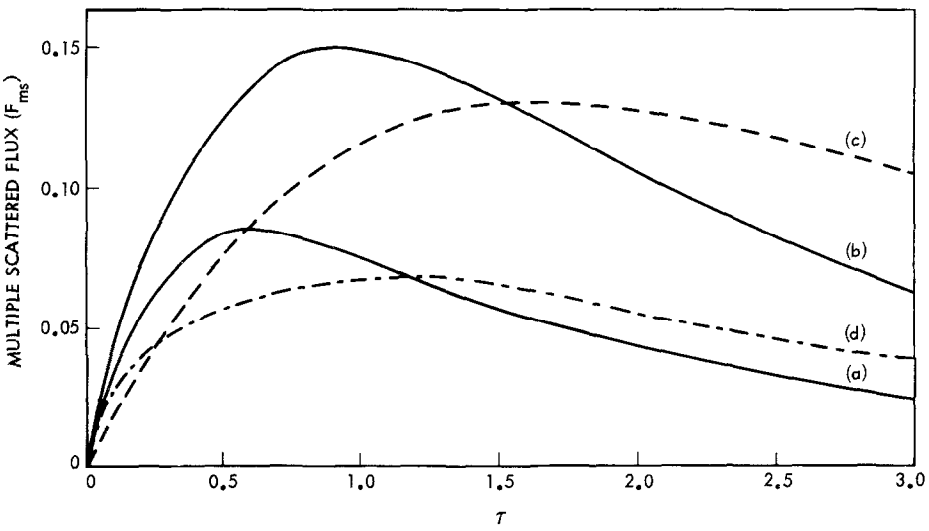

Fig. 7. A comparison between the multiple scattered flux in the plane-parallel approximation with the solution of the moment equations. Curves (a) and (b) represent the plane parallel multiply-scattered flux (as a function of τ) for $\mu_0 = 0.25$ and 0.5, respectively. The dashed curves (c) and (d) represents the average multiply-scattered flux over the nucleus surface in spherical geometry (Section 4), and plane parallel geometry (Section 5), respectively.

effective illumination angle. This is the method used by Weissman and Kieffer (1984a), who chose $\mu_0 = 0.3$. While it is clear that no one optimal μ_0 exists for which the plane parallel and the spherical solutions agree over a wide range of τ, over discrete intervals of τ the two solutions will agree with the correct choice of μ_0. For example, on comparing curves (a), (b) with (c), is clear that at $\tau = 0.5$ the fluxes are in good agreement for $\mu_0 = 0.25$, while $\tau = 1.5$ requires the cosine of the effective solar zenith angle to be increased to ≈ 0.5.

6. Discussion

With the recent satellite flyby missions to comet Halley, much has been learned about the more complex properties of the coma. For example, the coma morphology, dust jets, the nature of the dust grains, etc, are all properties about which a great deal of new insight has been gained (*Nature* **321**). Unfortunately, no direct measurement has yet been made of the total coma opacity. Any mention of the opacity of the coma entails a priori assumptions about the physical characteristics of the dust grains, e.g. their single scattering albedo (Keller *et al.*, 1986). One particular difficulty is the presence of discrete dust jets, which can be seen to be many times more optically thick than the surrounding area. Similarly, thermal models that incorporate hydrodynamical calculations to compute the opacity are subject to numerous assumptions such as the dust/gas ratio and the particle size distribution. Thus, instead of attempting to derive the opacity and the related heat flux at the surface

for particular comets, as was done in the past, a wide range of τ values was considered and the impinging flux at the nucleus subsequently studied. Although this study enables us better to understand the factors involved in the radiative transfer problem in spherical atmospheres, its application to comets is limited by its assumption that the dust density varies uniformly as $1/r^2$ around the nucleus. In reality, the dust density has been shown to be asymmetric with respect to latitude, and to depend on the rotation of the nucleus (Sekanina and Larson, 1986).

In the optically-thin limit, closed form expressions were derived describing the single scattered flux in a spherically symmetric atmosphere. From these analytical expressions it was seen that the 'forward shadow' region of the coma makes a significant contribution to the flux. Although the non-isotropic singly scattered flux was larger than in the isotropic case, the total flux resulting from the diffuse radiation fields in the coma, was shown to be a decreasing function of τ. In other words, it was always less than the unattenuated direct radiation obtained in the absence of a coma. Furthermore, on considering two different forms of the radial distribution of the dust, $1/r^2$ and $1/r^3$, the latter resulted in a smaller flux at least in the isotropic case. Since the $1/r^3$ distribution concentrates more dust in a smaller volume surrounding the nucleus, this result is in qualitative agreement with the results of the plane parallel approximation, in which the average flux was less than that obtained in the spherical $1/r^2$ distribution.

The application of the moment solution of Wilson and Sen (1980) to cometary atmospheres (Marconi and Mendis, 1984), was found to be somewhat restrictive; being defined only if $A = g = 0$. However, with these restrictions taken into account, the behaviour of the single scattered flux as function of τ and ψ was found to be in good agreement with the method described in Appendix A. For the isotropic multiple-scattering case, the downward-directed diffuse intensity I_3 was generally found to be a non-monotonic function of the radial height r. For example, for $\tau > 2.0$, I_3 attained its maximum a few kilometers above the nucleus, yielding a slightly lower value at the surface. Furthermore, at larger opacities the flux at the surface rapidly decreases with ψ, which in the case of comets, would result in a decreased dust production rate with ψ. However, in the region where the dust production rate – and, therefore, τ – is largest, it has been shown to possibly lead to a reduced energy flux; so that a negative feedback mechanism would be initiated. This would tend to make the surface more isothermal than would be the case if the coma were spherically symmetric, or if no coma were present. Most importantly, although this study was limited to isotropic scattering, the total flux impinging the nucleus was never found to be greater than πS, the direct flux in the absence of a coma.

Finally, the approximation where the spherical atmosphere was replaced locally at each ψ by plane parallel layers, was found to underestimate the flux for moderate to large τ. Over discrete intervals of τ the flux was slightly better approximated by choosing an effective μ_0. Nevertheless, the applicability of the plane parallel approximation is still somewhat restricted, since there is no one effective μ_0 which

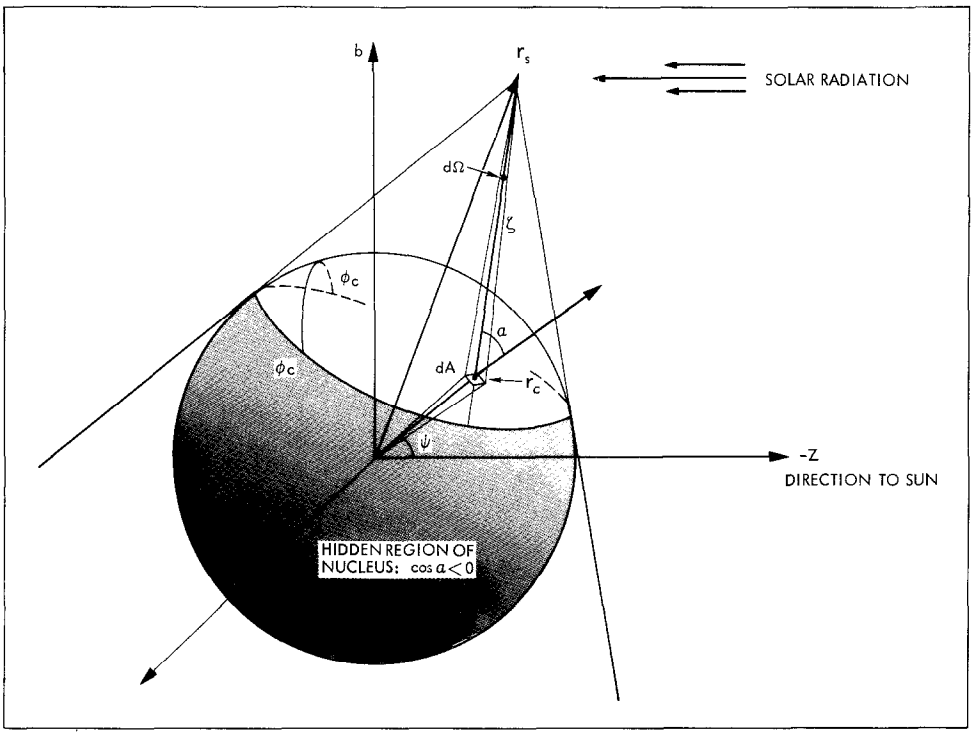

Fig. A1. The coordinate geometry used in the numerical integration of the single scattered flux.

could be chosen to represent the flux as a function of τ for a real spherical distribution of dust.

Acknowledgements

We are grateful to Dr R. Carlson, Dr R. West, and especially to Dr P. R. Weissman for their most helpful comments. This work was carried out while both authors held a National Research Council Resident Research Associateship at the Jet Propulsion Laboratory, California Institute of Technology, and was supported in part by the NASA Planetary Geology and Geophysics Program.

Appendix A: Calculation of the 'True' Single Scattered Flux as a Function of the Angle ψ

Consider a surface element $dA = R^2 \sin\psi \, d\psi \, d\phi$ on the nucleus, centered at the point $\mathbf{r}_c = (R \sin\psi \cos\phi, R \sin\psi \sin\phi, -R \cos\psi)$ (Figure A1). As seen from the point of scattering, $\mathbf{r}_s = (b, 0, z)$, it corresponds to a solid angle $d\Omega = dA \cos\alpha/\zeta^2$, where $\zeta = |\mathbf{r}_s - \mathbf{r}_c|$ and $\cos\alpha = \mathbf{r}_c \cdot (\mathbf{r}_s - \mathbf{r}_c)/(R\zeta)$. Here α is the angle between the outward directed normal at the point $\mathbf{r}_c$, and the direction where the point $\mathbf{r}_s$ is seen from the surface. If $\cos\alpha < 0$, this surface element is in the shadow of the nucleus as seen from the point $\mathbf{r}_s$.

The total flux falling onto the surface can be expressed as

$$\bar{F}_{ss} = 2\pi \int_0^{\pi} F_{ss}(\psi) R^2 \sin\psi \, d\psi, \tag{A1}$$

$$F_{ss}(\psi) = \int_{-\phi_c}^{\phi_c} \left\{ \int_{b=0}^{\infty} 2\pi \, b \, db \int_{z=-\infty}^{z_{max}} dz \; \frac{R\tau}{(z^2+b^2)} P(\mu) \exp\{-\tau_a - \tau_b\} \times \right.$$

$$\left. \times \frac{\cos\alpha}{4\pi \zeta^2} \right\} d\phi, \tag{A2}$$

where τ_a and τ_b denote the optical depths before and after scattering respectively, while $P(\mu)$ is the phase function. The integration limit on z, $z_{max} = \infty$ if $b > R$, and $z_{max} = -[R^2 - b^2]^{1/2}$ if $b \leq R$, excludes the backward shadow region, while the integration on ϕ is limited to the region where $\cos\alpha > 0$. In terms of cylindrical coordinates

$$\cos\alpha = (b\cos\phi\sin\psi - z\cos\psi - R)/\zeta, \tag{A3}$$

$$\zeta = \{(b - R\cos\phi\sin\psi)^2 + R^2\sin^2\phi\sin^2\psi + (z - R\cos\psi)^2\}^{1/2}; \tag{A4}$$

so that $\cos\alpha \geq 0$ if $\cos\phi \geq (R + z\cos\psi)/(b\sin\psi)$. The optical distance τ_a is according to Equation (7) given by

$$\tau_a = \frac{\tau R}{b}\left(\arctan\frac{z}{b} + \frac{\pi}{2}\right), \tag{A5}$$

while

$$\tau_b = \tau R \int_0^{\zeta} \frac{ds}{r^2}; \tag{A6}$$

where τ is the total optical thickness in the Sun-comet axis. The integration is carried out over the path after scattering, where the radius vector is $\mathbf{r} = \mathbf{r}_s + s(\mathbf{r}_c - \mathbf{r}_s)/\zeta$. Substituting for r^2 in Equation (A6) we obtain

$$\tau_b = \tau R \int_{s=0}^{\zeta} \frac{ds}{s^2 + ps + q} = \frac{2\tau R}{\sqrt{\Delta}}\left\{\arctan\left(\frac{p+2\zeta}{\sqrt{\Delta}}\right) - \right.$$

$$\left. - \arctan\left(\frac{p}{\sqrt{\Delta}}\right)\right\}, \tag{A7}$$

where

$$p = 2\mathbf{r}_s\cdot(\mathbf{r}_c - \mathbf{r}_s),$$

$$q = z^2 + b^2,$$

$$\Delta = 4q - p^2.$$

The cosine of the angle between incident and emerging light beams is simply

$$\mu = (\mathbf{r}_c - \mathbf{r}_s)/\zeta\cdot\hat{\mathbf{e}}_z = -(R\cos\psi - z)/\zeta,$$

which can be used as an argument in an arbitrary phase function.

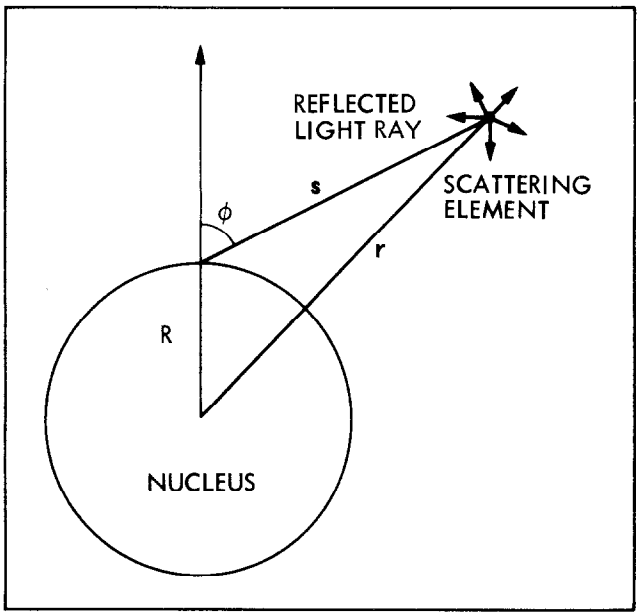

Fig. B1. The coordinate geometry used in obtained the fraction of reflected radiation scattered back from the atmosphere.

The single scattered flux calculated by using Equation (A2) is shown in Table I. It has also been used as an additional check for our generalization of the Marconi and Mendis (1984) solution.

Appendix B

Consider the case of a non-zero ground albedo. All the visible radiation that impinges the nucleus will not go into heating, a fraction AF of it, will be reflected back to be further scattered. If P represents the probability that a photon reflected from the surface returns to the nucleus, then the flux at the surface is given by the sum of the geometric progression

$$(1-A)F\,[1+AP+(AP)^2+\ \ldots] = \frac{(1-A)F}{(1-AP)}\,. \tag{B1}$$

The fraction of radiation scattered back from the coma depends on the angle between the direction of reflection and the outward directed surface normal (Figure B1). If this fraction is denoted $f(\phi)$, the total probability of return from the coma is given by the integral

$$P = 2\int_0^{\pi/2} f(\phi)\cos(\phi)\sin(\phi)\,\mathrm{d}\phi \tag{B2}$$

where the cos ϕ term implies a Lambert surface. To evaluate $f(\phi)$ we use the formula

$$f(\phi) = \int_0^\infty \tau R/r^2 \, (R^2/4r^2) \, ds, \tag{B3}$$

corresponding to the 'zeroth-order' approximation. Substituting $r^2 = s^2 + 2sR \cos \phi + R^2$ into Equation (B3) and integrating yields

$$f(\phi) = \frac{\tau}{8} \frac{1}{\sin^2 \phi} \left(\frac{\phi}{\sin \phi} - \cos \phi \right). \tag{B4}$$

Finally, on substituting Equation (B4) into (B2) we obtain the probability $P = (4 - \pi)/8 \, \tau \approx \tau/9$.

If we now consider the ratio of the total flux in the presence of a coma to that in the no coma case, the factor $(1 - A)$ in Equation (B1) cancels out. The increase in the flux due to the reflected photons scattered back from the atmosphere is therefore $(1 - AP)^{-1}$. For example, if $\tau = 1.0$ and $A = 0.04$, as observed for comet Halley (cf. Keller *et al.*, 1986), the increase in the flux is only $\approx 0.4\%$. Furthermore if the scattering were strongly forward-directed the probability would be even further reduced.

The simplicity of Equations (B2)–(B4) goes back to the fact that we have neglected multiple scattering and the attenuation by the atmosphere. However, although these equations strictly apply to the case $\tau \to 0$, Monte Carlo simulations have shown that the neglect of both these effects tend to negate each other so that the final result $P \approx \tau/9$ is a rather good approximation also for moderate and large τ's.

References

Fanale, F. P. and Savail, J. R.: 1984, *Icarus* **60**, 476.

Divine, N.: 1981, ESA SP-174, 25.

Hellmich, R. and Keller, H. U.: 1980, in I. Halliday and B. A. McIntosh (eds.), *Solid Particles in the Solar System*, D. Reidel, Dordrecht, Holland, pp. 255.

Hellmich, R.: 1981, *Astron. Astrophys.* **93**, 341.

Herman, G. and Podolak, M.: 1985, *Icarus* **61**, 252.

Irvine, W. M.: 1975, *Icarus* **25**, 175.

Keller, H. U., Arpigny, C., Barbieri, C., Bonnet, R. M., Cazes, S., Coradini, M., Cosmovici, C. B., Delamere, W. A., Huebner, W. F., Hughes, D. W., Jamar, C., Malaise, D., Reitsema, H. J., Schmidt, H. U., Schmidt, W. K. H., Seige, P., Whipple, F. L., and Wilhelm, K.: 1986, *Nature* **321**, 320.

Liou, K. N.: 1974, *J. Atmos. Sci.* **31**, 1473.

Marconi, M. L. and Mendis, D. A.: 1984, *Astrophys. J.* **287**, 445.

Sekanina, Z. and Larson, S. M.: 1986, *Astron. J.* **92**, 462.

Shettle, E. P. and Weinmann, J. A.: 1970, *J. Atmos. Sci.* **27**, 1048.

Sobolev, V. V.: 1975, *Light Scattering in Planetary Atmospheres* (transl. from Russian by W. M. Irvine), Pergamon Press, Elmsford, New York.

Squyres, S. W., McKay, C. P., and Reynolds, R. T.: 1985, *J. Geophys. Res.* **90**, 12381.

Weissman, P. R. and Kieffer, H. H.: 1981, *Icarus* **47**, 302.

Weissman, P. R. and Kieffer, H. H.: 1984a, *J. Geophys. Res.* **89**, C358.

Weissman, P. R. and Kieffer, H. H.: 1984b, *Adv. Space Res.* **4**, 221.

Wilson, S. J. and Sen, K. K.: 1980, *Astrophys. Space Sci.* **69**,107.

Wilson, S. J. and Wan, F. S.: 1983, *The Moon and the Planets* **29**, 1.